Available online at www.sciencedirect.com

ScienceDirect

Ceramics International 38 (2012) 125–130

CERAMICS INTERNATIONAL

www.elsevier.com/locate/ceramint

Preparation of $Sr_2SiO_4:Eu^{3+}$ phosphors by microwave-assisted sintering and their luminescent properties

Huang-Yu Chen [a], Min-Hang Weng [b], Shoou-Jinn Chang [a], Ru-Yuan Yang [c,*]

[a] *Institute of Microelectronics, Department of Electrical Engineering, Advanced Optoelectronic Technology Center, Center for Micro/Nano Science and Technology, National Cheng Kung University, Tainan 701, Taiwan*

[b] *Medical Devices and Opto-electronics Equipment Department, Metal Industries Research & Development Center, Taiwan*

[c] *Department of Material Engineering, National Pingtung University of Science and Technology, No. 1, Shuefu Road, Neipu, Pingtung County 912, Taiwan*

Received 26 May 2011; received in revised form 20 June 2011; accepted 23 June 2011

Abstract

An Eu^{3+} activated strontium silicate phosphor was synthesized using a microwave-assisted sintering with a flux NH_4Cl. X-ray powder diffraction analysis confirmed the formation of pure Sr_2SiO_4 phase without second phase or phases of starting materials as $Sr_{1.9}SiO_4:Eu^{3+}_{0.1}$ powders sintered at various temperatures in microwave furnace for 1 h. Scanning electron microscopy showed smaller particle size and more uniform grain size distributions are obtained by microwave-assisted sintering. In the PL studies, the excitation spectrum of $Sr_{1.9}SiO_4:Eu^{3+}_{0.1}$ phosphors exhibited a broad band in the UV region centered at about 270 nm which was consistent with the absorption spectra. Both microwave sintered and conventionally sintered powders emitted a maximum luminescence centered at 617 nm under excitation of 395 nm, with similar luminescent intensity. The results showed that microwave processing has the potential to decrease the sintering time and required energy input for the production of $Sr_{1.9}SiO_4:Eu^{3+}_{0.1}$ phosphors without degrading photoluminescence.

Keywords: A. Microwave processing; A. Sintering; C. Optical properties; D. Silicate; Phosphors

---

1. Introduction

White light emitting diodes (LEDs), with their characteristics of high brightness, reliability, long life time, low environmental impact and energy efficiency [1,2], are expected to replace conventional incandescent and fluorescent lamps in the near future. Recently, considerable efforts have been devoted to study on phosphors used for white LEDs [3–5]. The function of the phosphors is to absorb the ultraviolet (UV) or blue light and convert it to visible light. A potential phosphor should therefore have strong absorption and excitation in the region from ultraviolet to blue, and should emit the desired light. Many studies have been conducted to develop new oxide phosphors with high performance for phosphor applications [6,7].

In the past, Sr_2SiO_4 phosphor doped with Eu^{3+} has been prepared by means of a solid-state reaction using a conventional sintering furnace [8,9]. $Sr_2SiO_4:Eu^{3+}$ shows orange–red emission of Eu^{3+} substituted in two different Sr sites. However, longer sintering time and higher sintering temperature are required to synthesize the phosphor by means of a solid-state reaction. Furthermore, high temperature solid-state reactions usually generate agglomerate powders, which can easily change the structural characteristics of the powders [10]. To achieve a better quality of small particle size powders, an alternative sintering method referred to as microwave-assisted sintering was proposed using different heat generation and transfer mechanisms. Microwave-assisted sintering is fundamentally different from conventional sintering. In conventional sintering heat transfer takes place by radiation or conduction, and the heat energy is transferred from the sample surface to the core by conduction. In contrast, during microwave-assisted sintering procedure the whole of the sample absorbs microwaves and is heated by volumetric heating [11]. As a result, microwave-assisted sintering of materials has generally been

---

[*] Corresponding author. Tel.: +886 8 7703202x7555; fax: +886 8 7740552.
E-mail address: ryyang@mail.npust.edu.tw (R.-Y. Yang).

0272-8842/$36.00. Crown Copyright © 2011 Published by Elsevier Ltd and Techna Group S.r.l. All rights reserved.
doi:10.1016/j.ceramint.2011.06.044

found to reduce the required sintering time and temperatures [12–14], and achieve a rapid heating rate [15]. However, although microwave-assisted sintering has these advantages, there are few papers investigating the influence on the ceramic materials during sintering, especially in phosphor.

In this paper, we synthesized the Sr_2SiO_4 doped with Eu^{3+} phosphor materials using microwave-assisted sintering technique and discussed its microstructure and photoluminescent properties. The results showed that microwave-assisted sintering can reduce the formation temperature and obtain highly homogeneous phosphors, even in a short sintering time.

2. Experimental procedure

2.1. Samples preparation

$SrCO_3$, SiO_2, Eu_2O_3, and NH_4Cl with a purity of 99.9% were used as staring materials. $SrCO_3$, SiO_2, and Eu_2O_3 were mixed together by 1.9:1:0.05 mole ratio and 2 wt% NH_4Cl were added as a flux. The mixtures were mixed in alcohol as solvent and ball-milled for 1 h with zirconia balls. After drying, Eu^{3+} doped Sr_2SiO_4 phosphors were synthesized by means of a solid-state reaction method using microwave furnace to form $Sr_{1.9}SiO_4{:}Eu^{3+}{}_{0.1}$ powders. Fig. 1 shows the flow chart of the $Sr_{1.9}SiO_4{:}Eu^{3+}{}_{0.1}$ phosphors prepared by microwave assisted sintering. In the case of microwave-assisted sintering, a microwave furnace (Therm Wave Mod. III), with a continuously variable power of 2.45 GHz microwaves up to 1.3 kW, was used. Silicon carbide (SiC), having a very strong heating response to 2.45 GHz microwaves, was used as a susceptor to provide indirect heating for the powders [16]. The sample was placed on an Al_2O_3 crucible in a microwave cavity surrounded by four silicon carbide susceptors, and encapsulated by a ceramic fiber insulating material. The samples were sintered at 900, 1000, 1100 and 1200 °C for 1 h under an air atmosphere with a power of 900 ± 20 W, which produced an average heating rate greater than 100 °C/min. In order to compare to the performance prepared using conventional sintering, a sample was prepared using the same procedures, differing only in sintering at 1200 °C for 3 h in an air atmosphere, using a conventional sintering furnace.

2.2. Characterization

The crystalline phases of the phosphors were identified by X-ray diffraction (Bruker D8 Advance), analysis with CuKα radiation of $\lambda = 1.54$ Å using a Ni filter, and with a secondary graphite monochromator to realize the effect of the sintering process on the crystallization of the phosphors. A scan range of $2\theta = 20–80°$ with a step of 0.03° and 0.4 s as a count time per-step were used. Scanning electron microscopy (SEM; HORIBA EX-200), was used to observe the particle morphology of phosphors. Optical absorption spectra were measured at room temperature using a UV-vis spectrophotometer (V-600). The excitation and emission spectra were obtained using spectrofluorimeter (PL, JASCO FP-6000), equipped with a 150 W xenon lamp as the light source. To compare phosphor performance data accurately, specimens were measured within the same sample holder to ensure consistent amounts of phosphor materials in all samples in this study.

3. Results and discussion

3.1. Structure

Fig. 2 shows the X-ray diffraction patterns of $Sr_{1.9}SiO_4{:}Eu^{3+}{}_{0.1}$ sintered at various temperatures for 1 h in the microwave furnace. It has been reported that the crystal structures of α-Sr_2SiO_4 (orthorhombic), and β-Sr_2SiO_4 (monoclinic), are very similar, and the XRD peaks are therefore also similar in the JCPDS cards of both phases, and the both structures can co-exist [17,18]. From Fig. 2, the crystal

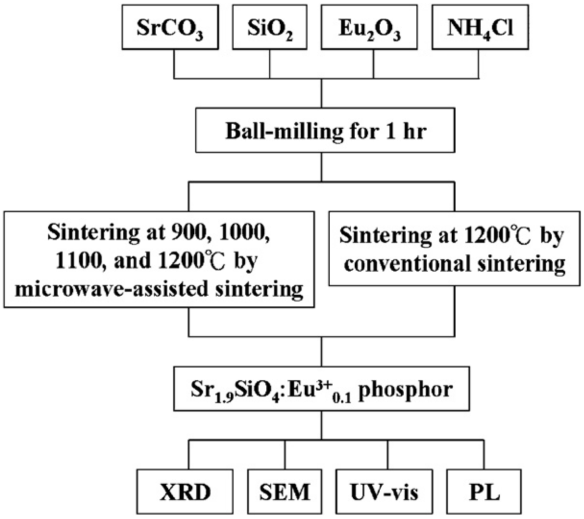

Fig. 1. Flow chart for the preparation of $Sr_{1.9}SiO_4{:}Eu^{3+}{}_{0.1}$ phosphors prepared by microwave-assisted sintering at various temperatures.

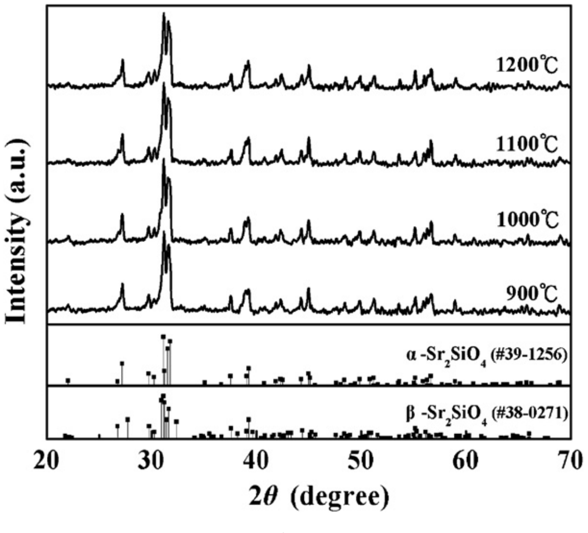

Fig. 2. XRD pattern of $Sr_{1.9}SiO_4{:}Eu^{3+}{}_{0.1}$ phosphors prepared by microwave-assisted sintering at various temperatures. The XRD JCPDS cards for monoclinic and orthorhombic phases of Sr_2SiO_4 are shown.

structure of the formed powder is major α-Sr_2SiO_4 (JCPDS #39-1256), without any impurities. No peaks of un-reacted $SrCO_3$ and SiO_2 are observed in XRD patterns, indicating that the reaction of raw materials is complete even at 900 °C. In this structure, Sr^{2+} ions located at two kinds of non-equivalent lattice sites, which coordination numbers are 9 and 10, respectively. Si^{4+} ions are located at the center of oxygen tetrahedron, and O^{2+} ions are located at three kinds of non-equivalent lattice sites, which space group is *Pmna*. When the Eu^{3+} ion is introduced into the Sr_2SiO_4 structure, it may readily substitute for Sr^{2+} sites since the ionic radii of ${Eu_{IX}}^{3+}$ (~1.30 Å), and ${Eu_X}^{3+}$ (~1.35 Å), almost approach those of ${Sr_{IX}}^{2+}$ (~1.31 Å), and ${Sr_X}^{2+}$ (~1.36 Å). The crystal structure experienced no change as Eu^{3+} ion doped, which can be seen from Fig. 2. The average crystal size can be calculated from the full width at half maximum (FWHM), of the X-ray diffraction peak using Scherrer's equation [19]:

$$D = \frac{K\lambda}{B\cos\theta} \qquad (1)$$

where D is the crystal size, λ is the X-ray wavelength, B is the FWHM of a diffraction peak and the peak of (2 1 1) is used in our case, θ is the diffraction angle, and K is the Scherrer's constant of the order of unity for usual crystals [19]. The calculated size of our specimens is similar as sintering temperature increases from 900 to 1200 °C, ranging from 25 to 27 nm. The Sr_2SiO_4:Eu phosphor synthesized by sol–gel method was investigated by Hsu et al. [20]; it showed that pure Sr_2SiO_4 phase was found in sintering temperatures between 1100 and 1300 °C for 1 h, indicating that there were still un-reacted raw materials observed below 1000 °C. It has been known that the sintering temperature of complex oxide ceramics using a sol–gel technique is relatively low, and a highly homogeneous ceramic powder can be obtained. However, in this paper, the $Sr_2SiO_4:Eu^{3+}$ phosphor synthesized by microwave-assisted sintering with a flux NH_4Cl can obtain pure Sr_2SiO_4 phase even though the sintering temperature is 900 °C. The result shows that the formation temperature of Sr_2SiO_4 using microwave-assisted sintering method with a flux NH_4Cl is relatively lower than when using a sol–gel technique. Furthermore, microwave-assisted sintering used a power level of 900 W, corresponding to a heating rate about 100 °C/min, and conventional sintering used a heating rate of 10 °C/min, indicating the sintering time of Sr_2SiO_4:Eu phosphors can be reduced due to fast heating rate, reducing sintering time when the microwave-assisted sintering method is used.

3.2. Morphology

Fig. 3 shows the SEM images of $Sr_{1.9}SiO_4:{Eu^{3+}}_{0.1}$ sintered at various temperatures for 1 h in the microwave furnace. The shape of the particles is not much different from each other, but the grain size increases significantly as sintering at higher temperature. Synthesis of $Sr_2SiO_4:Pr^{3+}$ phosphors using a conventional solid-state reaction was investigated by Zhang et al. [21], showing that the shape of $Sr_2SiO_4:Pr^{3+}$ phosphor grain is irregular with observable porosity for high temperature of thermal decomposition, and the grain size is in a wide distribution with average size of 50–200 μm. However, grain sizes are relatively small for microwave-assisted sintered powders, as seen in Fig. 3. The average grain size of them is about 1–2 μm even if the sintering temperature is 1200 °C. In other materials systems, it also been observed that the samples sintered by microwave-assisted sintering have smaller grains than those produced by the conventional process [22]. In the grain growth process, the ions jump from the convex to the concave side of the grain boundaries, but microwave-assisted sintering seems not to facilitate such a process, resulting in a smaller grain microstructure [22]. Additionally, the grain size distribution of the microwave-assisted sintered powder is uniform without aggregation. The reason for this is that when materials interact with microwave power the heat is generated within the material itself, then dispersed uniformly within the material [12].

3.3. Absorption spectrum

Fig. 4 shows the absorption spectra of $Sr_{1.9}SiO_4:{Eu^{3+}}_{0.1}$ phosphors sintered at various temperatures for 1 h in a microwave furnace. A strong absorption peak is located in the UV range at ~250 nm, corresponding to the valence-to-conduction band transitions of the Sr_2SiO_4 host lattice. The absorption intensities increase as sintering temperature increases. It was known that the increase of sintering temperatures contributed to the enhancement of the preference of substitutional Eu^{3+} ions [23]. It can therefore be concluded that the increasing absorption intensities may be attributed to better substitution of Eu^{3+} ions in Sr_2SiO_4 due to higher sintering temperature. Several weak peaks can also be seen in the range of 370–500 nm from the absorption spectra of samples sintered at different temperatures, originating from the photon absorption by the outer electron as the $4f \rightarrow 5d$ transition takes place [24].

3.4. Excitation and emission spectrum

Fig. 5 shows the excitation spectra of the red emission at 617 nm of $Sr_{1.9}SiO_4:{Eu^{3+}}_{0.1}$ phosphors sintered at various temperatures for 1 h in a microwave furnace, in the spectral region from 200 to 450 nm. The spectrum of $Sr_{1.9}SiO_4:{Eu^{3+}}_{0.1}$ phosphors exhibit a broad band in the UV region centered at about 270 nm, and several sharp lines between 300 and 450 nm. The broad absorption band is referred to as a charge transfer state (CTS) band due to the europium–oxygen interactions, which are caused by an electron transfer from an oxygen 2p orbital to an empty 4f shell of europium. The sharp excitation peaks located at 319, 363, 383, 395, and 416 nm are related to the intraconfigurational 4f–4f transitions of Eu^{3+} ions in the host lattices, which can be assigned to ${}^7F_0 \rightarrow {}^5H_6$, ${}^7F_0 \rightarrow {}^5D_4$, ${}^7F_0 \rightarrow {}^5L_7$, ${}^7F_0 \rightarrow {}^5L_6$, and ${}^7F_0 \rightarrow {}^5D_3$ transitions, respectively. The peak positions are in good agreement with the excitation spectra reported in Refs. [8,10]. The excitation spectra indicate that the intensities of both CTS and intra-4f transition increase as sintering temperature increases. The excitation spectrum

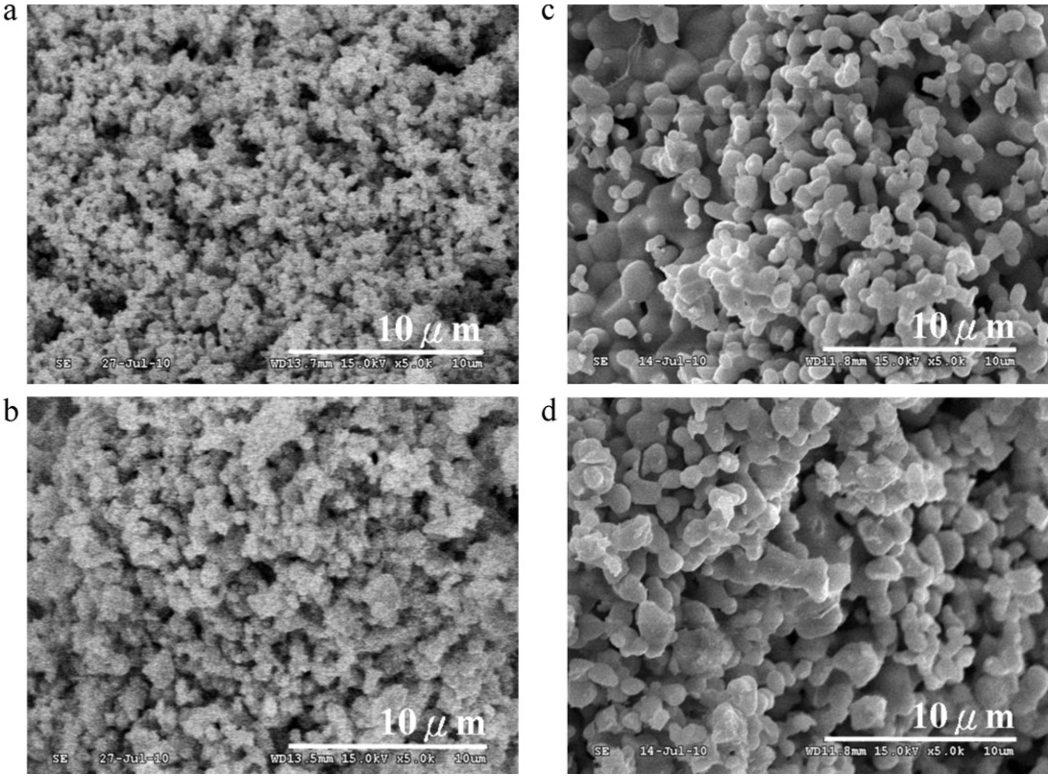

Fig. 3. SEM images of $Sr_{1.9}SiO_4:Eu^{3+}_{0.1}$ phosphors prepared by microwave-assisted sintering at (a) 900 °C, (b) 1000 °C, (c) 1100 °C, and (d) 1200 °C for 1 h.

consists of a broad band with a maximum at around 270 nm due to the europium–oxygen interactions, agreeing well with the absorption spectra (Fig. 4).

Fig. 6 shows the emission spectra of $Sr_{1.9}SiO_4:Eu^{3+}_{0.1}$ phosphors prepared by microwave-assisted sintering at various temperatures for 1 h. $Sr_{1.9}SiO_4:Eu^{3+}_{0.1}$ phosphor is excited with 395 nm wavelength from a xenon lamp. The emission wavelengths are all in the red region, corresponding to 592 nm ($^5D_0 \rightarrow {}^7F_1$), 620 nm ($^5D_0 \rightarrow {}^7F_2$), 654 nm ($^5D_0 \rightarrow {}^7F_3$), and 704 nm ($^5D_0 \rightarrow {}^7F_4$) [8,10], respectively. Obviously, the strong emission of Eu^{3+} is also due to an efficient energy transfer from the host lattice to Eu^{3+} in $Sr_{1.9}SiO_4:Eu^{3+}_{0.1}$ powders. As the sintering temperature increases, the emission intensity is increased. However, Nag et al. [9] previously synthesized $Sr_2SiO_4:Eu^{3+}$ phosphors by means of a solid-state reaction and observed an intense emission peak at 575 nm, which is not found in Fig. 6. According to the research of Bacce et al. [25], the intense emission at 575 nm was ascribed to the Eu^{3+} ions located in the lattice interstices and associated with an oxide ion not bound to silicon, such as $[Eu^{3+} \leftarrow O^{2-}]$ interstitial defects. It is therefore suggested that no interstitial defects existed in the $Sr_2SiO_4:Eu^{3+}$ phosphors prepared by microwave-assisted sintering with a flux NH_4Cl, indicating that this method has the potential advantages of improving sintering and decreasing the defects which may appear during the sintering process. However, there is still another possible

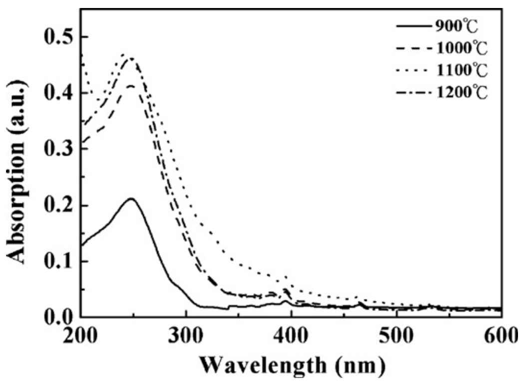

Fig. 4. The absorption spectra of $Sr_{1.9}SiO_4:Eu^{3+}_{0.1}$ phosphors sintered at various temperatures for 1 h in microwave furnace.

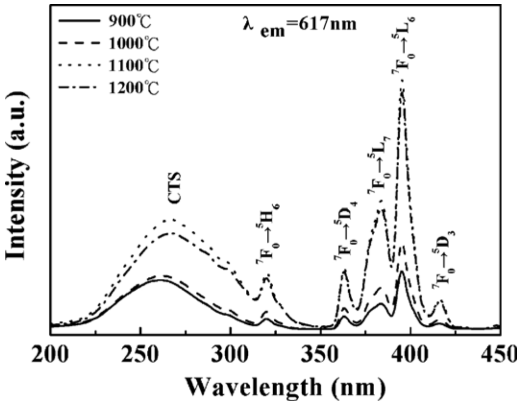

Fig. 5. Photoluminescence excitation spectra of $Sr_{1.9}SiO_4:Eu^{3+}_{0.1}$ phosphors prepared by microwave-assisted sintering at various temperatures ($\lambda_{em} = 617$ nm).

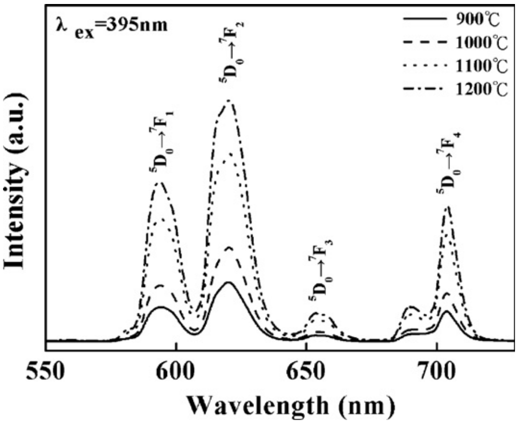

Fig. 6. Photoluminescence emission spectra of $Sr_{1.9}SiO_4:Eu^{3+}{}_{0.1}$ phosphors prepared by microwave-assisted sintering at various temperatures (λ_{ex} = 395 nm).

explanation for the absence of the 575 nm emission. Since the $^5D_0 \rightarrow {}^7F_0$ transition of Eu^{3+} is forbidden by both electric-dipole and magnetic-dipole selection rules, indicating only weak or no emission peak can be detected.

Fig. 7 shows the emission spectra of the $Sr_{1.9}SiO_4:Eu^{3+}{}_{0.1}$ phosphors prepared by microwave-assisted sintering at 1200 °C for 1 h and conventional sintering at 1200 °C for 3 h, respectively. Even if only 1 h of sintering time is used, it is shown that $Sr_{1.9}SiO_4:Eu^{3+}{}_{0.1}$ phosphor prepared by microwave-assisted sintering has a similar luminescent intensity to that prepared by conventional sintering. This means that microwave-assisted sintering may be able to reduce the sintering time and cost of producing high-quality phosphors. Furthermore, no emission peak is located at 575 nm observed in conventionally sintered $Sr_{1.9}SiO_4:Eu^{3+}{}_{0.1}$ phosphor. The strong and narrow emission feature is indicative of the presence of europium ions in the orthorhombic structure of Sr_2SiO_4. It is well-known that the $^5D_0 \rightarrow {}^7F_1$ transition is magnetic dipolar in character and is independent of the crystal fields, unlike the $^5D_0 \rightarrow {}^7F_0$, which is a weak electric dipole transition. Although the $^5D_0 \rightarrow {}^7F_0$ transition is forbidden in a centrosymmetric environment, it is allowed in low-symmetry sites. This effect is evidenced by the complete disappearance of the $^5D_0 \rightarrow {}^7F_0$ transition in the emission spectra of Fig. 7. Furthermore, the ratio of the relative intensities of the $^5D_0 \rightarrow {}^7F_2$ and $^5D_0 \rightarrow {}^7F_1$ transitions, which is used as a reliable spectroscopic probe for the degree of symmetry around the Eu^{3+} ion, is around 2.4 compared with the typical value of higher than 3, which is characteristic of low-symmetry sites [26]. These observations constitute a further demonstration that the Eu^{3+} ions are embedded in their crystalline surroundings [27].

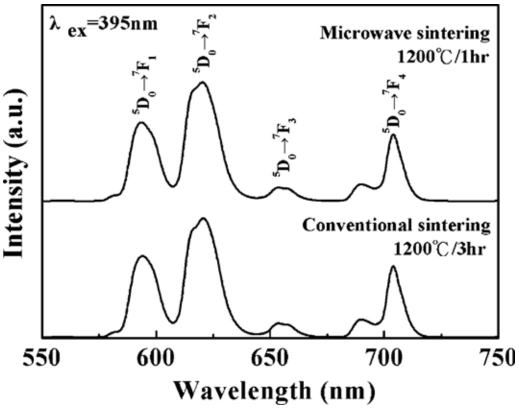

Fig. 7. Photoluminescence emission spectra of $Sr_{1.9}SiO_4:Eu^{3+}{}_{0.1}$ phosphors prepared by different sintering methods (λ_{ex} = 395 nm).

4. Conclusion

In this paper we synthesize $Sr_{1.9}SiO_4:Eu^{3+}{}_{0.1}$ phosphors using microwave-assisted sintering with 2 wt% flux NH_4Cl. It is revealed that compared to conventional sintering, a relatively low temperature of 900 °C is required to form the single phase of Sr_2SiO_4 using microwave-assisted sintering. Since $Sr_{1.9}SiO_4:Eu^{3+}{}_{0.1}$ phosphors are sintered under microwaves, a pronouncedly smaller and more uniform grain size of 1–2 μm is obtained, as required in white LEDs applications. Furthermore, the emission intensity of $Sr_{1.9}SiO_4:Eu^{3+}{}_{0.1}$ phosphors using microwave-assisted sintering is similar to that using conventional sintering, even if the sintering time is only 1 h. Consequently, microwave-assisted sintering may have good potential for producing the high-quality $Sr_{1.9}SiO_4:Eu^{3+}{}_{0.1}$ phosphors applied in white LEDs.

Acknowledgements

The authors would like to acknowledge Mr. Y.K. Yang for preparing the samples. The authors would also like to acknowledge funding support from the Nation Science Council of Taiwan, under Grant NSC 98-2221-E-020-017, and from the Ministry of Economic Affairs of Taiwan under Grant NTC 100-EC-17-A-01-05-0642, and would also like to acknowledge National Nano Device Laboratories for supporting the experimental equipment.

References

[1] S. Yao, D. Chen, Combustion synthesis and luminescent properties of a new material $Li_2(Ba_{0.99},Eu_{0.01})SiO_4:B^{3+}$ for ultraviolet light emitting diodes, Opt. Laser Technol. 40 (2008) 466.

[2] R.J. Xie, H. Naoto, M. Mamoru, S. Ken, K. Naoki, Wavelength-tunable and thermally stable Li-α-sialon:Eu^{2+} oxynitride phosphors for white light-emitting diodes, Appl. Phys. Lett. 89 (2006) 241103.

[3] S. Kubota, H. Hara, H. Yamane, M. Shimada, Luminescent property of Eu^{3+} in a new compound, $(Sr_{0.99}La_{1.01})Zn_{0.99}O_{3.495}$, J. Electrochem. Soc. 149 (2002) H68.

[4] S. Ekambaram, K.C. Patil, M. Maaza, Synthesis of lamp phosphors: facile combustion approach, J. Alloys Compd. 393 (2005) 81–92.

[5] J.S. Kim, P.E. Jeon, J.C. Choi, H.L. Park, Emission color variation of $M_2SiO_4:Eu^{2+}$ (M = Ba, Sr, Ca) phosphors for light-emitting diode, Solid State Commun. 133 (2005) 187.

[6] Q.Y. Zhang, K. Pita, W. Ye, W.X. Que, Influence of annealing atmosphere and temperature on photoluminescence of Tb^{3+} or Eu^{3+}-activated zinc silicate thin film phosphors via sol–gel method, Chem. Phys. Lett. 351 (2002) 163–170.

[7] K.Y. Kim, H.K. Jung, H.D. Park, D. Kim, High luminance of new green emitting phosphor, Mg_2SnO_4:Mn, J. Lumin. 99 (2002) 169–173.

[8] Y. Qiao, X. Zhang, X. Ye, Y. Chen, H. Guo, Photoluminescent properties of $Sr_2SiO_4:Eu^{3+}$ and $Sr_2SiO_4:Eu^{2+}$ phosphors prepared by solid-state reaction method, J. Rare Earths 27 (2009) 323–326.

[9] A. Nag, T.G.N. Kutty, The light induce valence change of europium in Sr_2SiO_4:Eu involving transient crystal structure, J. Mater. Chem. 14 (2004) 1598–1604.

[10] J. Dhanaraj, R. Jagannathan, T.G.N. Kutty, C.H. Lu, Photoluminescence characteristics of $Y_2O_3:Eu^{3+}$ nanophosphors prepared using sol–gel thermolysis, J. Phys. Chem. B 105 (2001) 11098–11105.

[11] G. Prabhu, A. Chakraborty, B. Sarma, Microwave sintering of tungsten, Int. J. Refract. Met. Hard Mater. 27 (2009) 545–548.

[12] Z.P. Xie, X.D. Fan, Y. Huang, Accelerated sintering and phase transformation of TiO_2 in microwave radiation, J. Mater. Res. 13 (1998) 3417–3422.

[13] S. Ananthakumar, G. Krishnapriya, A.D. Damodaran, K.G.K. Warrier, Thermal decomposition characteristics of boehmite gels under microwave heating and associated microstructural features, Mater. Lett. 35 (1998) 95–99.

[14] S.A. Nightingal, D.P. Dunne, H.K. Worner, Sintering and grain growth of 3 mol% yttria zirconia in a microwave field, J. Mater. Sci. 31 (1996) 5039–5043.

[15] D.K. Agrawal, Microwave processing of ceramics, Curr. Opin. Solid State Mater. Sci. 3 (1998) 480–485.

[16] P.D. Ramash, D. Brandom, L. Schachter, Use of partially oxidized SiC particle bed for microwave sintering of low loss ceramics, Mater. Sci. Eng. A 266 (1999) 211–220.

[17] M. Catti, G. Gazzoni, G. Ivaldi, Structures of twinned β-Sr_2SiO_4 and of α'-$Sr_{1.9}Ba_{0.1}SiO_4$, Acta Crystallogr. C 39 (1983) 29–34.

[18] B.G. Hyde, J.R. Sellar, L. Stenberg, The $\beta \rightleftarrows \alpha'$ transition in Sr_2SiO_4 (and Ca_2SiO_4, K_2SeO_4 etc.), involving a modulated structure, Acta Crystallogr. B 42 (1986) 423–429.

[19] L.S. Birks, H. Friedman, Particle size determination from X-ray line broadening, J. Appl. Phys. 17 (1946) 687.

[20] W.H. Hsu, M.H. Sheng, M.S. Tsai, Preparation of Eu-activated strontium orthosilicate ($Sr_{1.95}sio_4:Eu_{0.05}$) phosphor by a sol–gel method and its luminescent properties, J. Alloys Compd. 467 (2009) 491–495.

[21] L. Zhang, X. Zhou, H. Zeng, H. Chen, X. Dong, White-light long-lasting phosphor $Sr_2SiO_4:Pr^{3+}$, Mater. Lett. 62 (2008) 2539–2541.

[22] C.Y. Tsay, K.S. Liu, I.N. Lin, Microwave sintering of $(Bi_{0.75}Ca_{1.2}Y_{1.05})(V_{0.6}Fe_{4.4})O_{12}$ microwave magnetic materials, J. Eur. Ceram. Soc. 24 (2004) 1057–1061.

[23] J.H. Lee, Y.J. Kim, Photoluminescent properties of $Sr_2SiO_4:Eu^{2+}$ phosphors prepared by solid-state reaction method, Mater. Sci. Eng. B 146 (2008) 99–102.

[24] G. Blasse, B.C. Grabmaier, Luminescent Materials, vol. 13, Springer-Verlag, Berlin/Heidelberg, 1994.

[25] E.D. Bacce, A.M. Pires, M.R. Davolos, Influence of Zn^{2+} co-doping ion on Eu^{3+}–O^{2-} associate luminescence in Sr_2SiO_4, J. Alloys Compd. 344 (2002) 312–315.

[26] G. Pucker, K. Gatterer, H.P. Fritzer, Optical investigation of Eu^{3+} in a sodium borosilicate glass: evidence for two different site distributions, Phys. Rev. B 53 (1996) 6225–6234.

[27] B.N.S. Bhaktha, C. Kinowski, M. Bouazaoui, B. Capoen, O. Robbe-Cristini, F. Beclin, P. Roussel, M. Ferrari, S. Turrell, Controlled growth of SnO_2 nanocrystals in Eu^{3+}-doped SiO_2–SnO_2 planar waveguides: a spectroscopic investigation, J. Phys. Chem. C 113 (2009) 21555–21559.